Exploring the utility of axial lumbar MRI for automatic diagnosis of intervertebral disc abnormalities

Subarna Ghosh[a], Vipin Chaudhary[a], Gurmeet Dhillon[b]
{sghosh7, ralomari, vipin}@buffalo.edu {gdhillon}@proscan.com
[a]University at Buffalo, SUNY, Buffalo, NY 14260
[b]ProScan Imaging of Buffalo, Williamsville, NY 14221

ABSTRACT

In this paper, we explore the importance of axial lumbar MRI slices for automatic detection of abnormalities. In the past, only the sagittal views were taken into account for lumbar CAD systems, ignoring the fact that a radiologist scans through the axial slices as well, to confirm the diagnosis and quantify various abnormalities like herniation and stenosis. Hence, we present an automatic diagnosis system from axial slices using CNN(Convolutional Neural Network) for dynamic feature extraction and classification of normal and abnormal lumbar discs. We show 80.81% accuracy (with a specificity of 85.29% and sensitivity of 75.56%) on 86 cases (391 discs) using only an axial slice for each disc, which implies the usefulness of axial views for automatic lumbar abnormality diagnosis in conjunction with sagittal views.

Keywords: CAD, Lumbar MRI, intervertebral disc abnormality, Convolutional Neural Networks

1. INTRODUCTION

In the recent years there has been a lot of research in the direction of automatic diagnosis of abnormalities from various imaging modalities like X-rays, CT[1,2] and MRI .[3–7] Efforts are being made to introduce computer-aided diagnosis results within the workflow of a radiologist along with the existing PACS (Picture Archiving and Communication System) system to tackle the severe shortage of radiologists[8] and to reduce the average time for diagnosis.

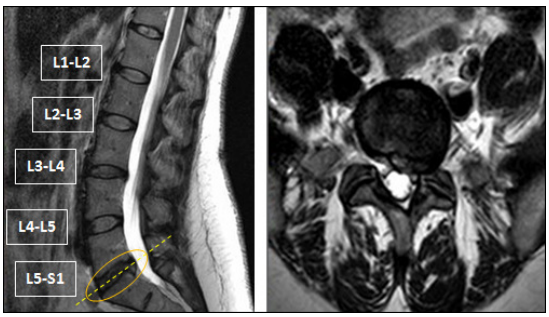

Figure 1: (Left) Sagittal view of a lumbar MRI showing an L5-S1 disc herniation and (Right) the corresponding axial view of the lumbar MRI confirming a left sided herniation.

Currently MR imaging with its numerous modalities is the most accurate non-invasive imaging technique to diagnose and quantify disc abnormalities.[9] Since 3D MRIs are too expensive, they are mostly used for research purposes while clinical MRIs are usually 2D. Most of the automatic diagnosis research based on clinical MRI data, however, uses only the sagittal views, even though radiologists usually scan through both the sagittal and the axial to make his final diagnosis. It is evident from Fig. 1, that while the sagittal slice(left) shows herniation in disc L5-S1, the axial view confirms the diagnosis and can also be used for quantification of the herniation. Moreover, the reason scientists have used only sagittal slices for automatic diagnosis is that, not only are they

simpler in terms of image processing than the axial views, it is also very challenging to select a relevant axial image out of multiple slices per disc. Hence, we try to explore ways in which axial views can be processed and used to extract features for automatic diagnosis of lumbar abnormalities.

2. RELATED WORK

There has been a growing interest in the research community for automatic diagnosis of abnormalities from lumbar MRI. Tsai et al.[3] detected herniation from 3D MRI and CT volumes of the discs by using geometric features like shape, size and location. Michopoulou et al.[4] perform semi-automatic atlas-based intervertebral disc segmentation by fuzzy-c means and classified them into normal or degenerated using a Bayesian clssifier. They achieved 86-88% accuracy on 34 cases. They also reported 94% accuracy for a normal vs. degenerated discs classifier using texture features[10] from 50 manually segmented discs. Alomari et al.[5] presented a dessication diagnosis system from clinical lumbar MRI using a probabilistic model and they achieve over 96% accuracy. We have also proposed computer-aided diagnosis of herniation using heterogeneous classifiers[6] and composite features;[7] and achieve upto 98.29% accuracy and 96.23% sensitivity using a concatenation of Raw+LBP+Gabor+GLCM+Shape+Intensity features and PCA for dimensionality reduction on 35 cases.

In most of the previous work involving 2D clinical MRIs, only the mid-sagittal slice or three middle slices were taken into account, due to which left or right-sided disc abnormalities could have been missed. Moreover from radiologists' reports we observe that he scans through the axial MRI slices to localize and quantify disc herniation, degeneration and stenosis. This motivates us to perform comprehensive experiments for automatic diagnosis of inter-vertebral disc abnormalities from the axial slices, and hence explore their effectiveness in CAD systems.

3. PROPOSED APPROACH

3.1 Dataset

Clinical data used by our research group is procured in Proscan using a 3T Philips Medical Systems MRI scanner. It consists of manually coregistered T2 and T1 weighted sagittal views and T2 weighted axial views. Observing the clinical MRIs, we see that the technician acquires 6 axial slices for each lumbar intervertebral disc, changing the angle according to the orientation of the disc as we can see the L5-S1 axial slice in Fig 1. Depending upon the case, axial views of 4 or 5 discs are recorded starting from L5-S1 and ending in either L2-L3 or L1-L2 giving rise to 24 or 30 axial slices. We randomly pick 86 anonymized cases (a total of 391 discs with axial views), all of which have one or more lumbar disc abnormalities.

According to the radiologist's report (which we treat as ground truth), there are a total of 103 herniated discs, 48 bulging discs, 42 desiccated discs, 81 degenerated discs and 104 disc levels having mild to severe stenosis. If a disc level does not have any of the above abnormalities, then we label it as normal, else abnormal. We have a total of 201 normal discs. Another observation is that the 3rd and the 4th axial slices of each disc run through the nucleus and are the most helpful for diagnosis, localisation and quantification. In the next section (Sec. 3.2) we describe the steps for ROI(Region of Interest) extraction from an axial image.

3.2 ROI(Region of Interest) Extraction

The first step in our approach is to roughly localize the disc in the axial MRI slice (Fig. 2(a)). We see that for all patients the sagittal slices run from left to right covering the entire disc as shown in Fig. 2(b). Hence, we use the lines of intersection of the left-most and right-most sagittal-slices with the corresponding axial slice to create a rough bounding box (Fig 2(c)). Then, we empirically cut out top and bottom one-fourth of the image (Fig 2(d)) and finally go through a round of blurring and sharpening the image to reduce noise. We use the final localized image for feature extraction and classification as described in the subsequent sections.

3.3 Feature Extraction and Classification

In this section we discuss the design and specifics of CNN (Convolutional Neural Network) that we have used for automatic feature extraction and classification of lumbar discs in our experiments.

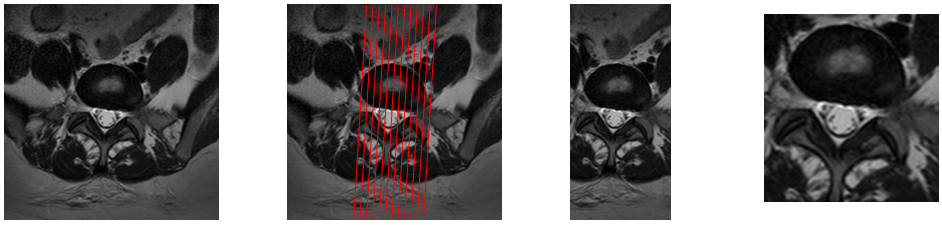

(a) (b) (c) (d)

Figure 2: Automatic ROI extraction from axial slice: (a) shows the original axial image, (b) shows the lines of intersection of the sagittal slices with the axial, (c) shows the rough ROI extracted using the left-most and right-most sagittal lines and (d) shows the final ROI.

3.3.1 Introduction to CNN

A Convolutional Neural Network (CNN)[11] is a multi-layer architechture trained in supervised mode using gradient-based methods. All the layers are trained simultaneously to minimize an overall objective function, hence the feature extraction is an integral part of the classification system. They are designed in such a way that successive layers learn progressively higher level features, until the last layer which produces categories. They have been shown to automatically learn salient image features and yield good recognition accuracy. Moreover they can be trained via a slightly modified back propagation, which makes implementation simple.[12]

3.3.2 Conceptual details

The feature extraction front end can be seen as composed of a stack of convolution(C-) and sub-sampling(S-) layers (Fig. 3). In general, at the convolution layer we have :

$$x_j^l = f(\sum_{i \in M_j} x_i^{l-1} * k_{ij}^l + b_j^l) \tag{1}$$

where x_j^l is the j-th output feature map in layer l and M_j is a selection of input maps in layer $l-1$, f is a non-linear function (a hyperbolic tangent or sigmoid), and b is a scalar bias. On each C-layer, multiple convolution kernels can be used, creating several different feature maps.

A subsampling layer produces downsampled versions of the input maps as:

$$\mathbf{x}_j^l = f(\beta_j^l down(\mathbf{x}_j^{l-1}) + b_j^l) \tag{2}$$

where $down(\cdot)$ represents a sub-sampling function. Each output map is given its own multiplicative bias β and an additive bias b. This results in a feature map of lower resolution where some position information about features has been eliminated, thereby building some level of distortion invariance in the representation.

The last 2 layers are usually linear classifiers eg. MLPs(Multi-Layer Perceptrons) operating on the feature representation extracted by the previous layers.

3.3.3 Our CNN design

Our CNN has 7 layers; 2 sub-sampling(S) layers, 3 convolutional(C) layers and 2 fully-connected (MLP) layers (Fig. 3). We resize all the axial images (obtained in Sec. 3.2) to 64x64 and then zero-pad them resulting in 74x74 images. These padded images are input to the first layer of the CNN, which is a C layer with 6 convolution kernels of size 11x11, resulting in 6 feature maps. The second layer is an S layer, and the third is a C layer with 16 kernels of size 11x11. The forth layer is a S layer, and the fifth is a C layer with 120 kernels of size 11x11. Both the S layers in our design have sub-sampling rates of 2. We design the CNN so that the fifth layer results in multiple 1x1 output maps which can be fed to the next layer similar to a Multi-Layer Perceptron. The sixth layer (fully-connected) has 84 neurons and the last layer has 2 output neurons. Connection between

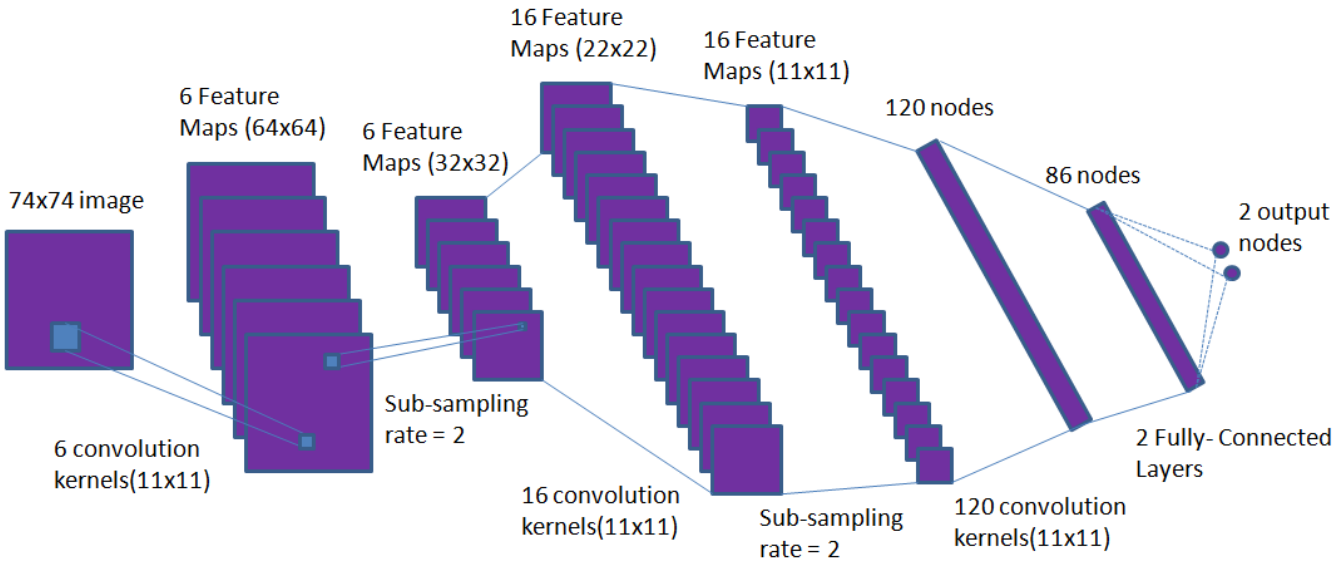

Figure 3: This figure shows a graphical depiction of our CNN used to classify intervertebral discs as normal or abnormal. The lower-layers are composed of alternating convolution and sub-sampling layers. The last two layers are fully-connected and correspond to an MLP(Multi-Layer Perceptron).

the S and C layers maynot be full, i.e an output feature maynot be a result of convolution of all the available input feature maps. We define two kinds of connection maps : Fully-connected is one where all the input feature maps are connected to an output feature map; and Randomly-connected, is where we generate the connection map randomly.

4. EXPERIMENTS AND RESULTS

4.1 Experimental Setup

We conduct 5-fold cross-validation experiments, so that there is no overlap of the training and tesing images. We have four sets of experiments 1)Slice 3 as input and a Fully-connected map, 2) Slice 3 as input and a Randomly-connected map, 3)Slice 4 as input and a Fully-connected map, 4) Slice 4 as input and a Randomly-connected map.

4.2 Metrics

The performance metrics, specificity and sensitivity are defined as follows :

$$\text{Specificity} = \frac{\text{TNs}}{\text{TNs} + \text{FPs}} \quad \text{Sensitivity} = \frac{\text{TPs}}{\text{TPs} + \text{FNs}} \tag{3}$$

where TNs is the Number of True Negatives, FNs is the Number of False Negatives, TPs is the Number of True Positives. FPs is the Number of False Positives.

4.3 Results and Discussion

We present our classification results of all four experiments in Table 1.

Classification accuracy of nearly 81% shows that the CNN is capable of extracting relevant features automatically from the challenging axial MRI images. CNN requires a huge number of training images. Thousands of training images have been used for tasks like character recognition,[11] whereas currently we have trained our CNN on 312 images. We could potentially get much better performance using a lot more training images, since we have access to thousands of clinical MRI.

Table 1: CNN performance results for 5-fold cross validation (Sec. 4)

Expt No.	Accuracy	Specificity	Sensitivity
1	77.75	81.09	74.21
2	80.81	85.29	75.56
3	75.70	79.60	71.58
4	78.77	80.60	76.84

5. CONCLUSION

We have proposed the design of a CNN (convolutional neural network), that detects disc abnormality from T2-weighted axial MRI with an accuracy of 81%. As far as our literature survey goes, there is hardly any previous work using axial views of clinical 2D MRIs. Our results show that there is useful information in the axial views, that can be automatically extracted using a CNN and hence motivates us to conduct more research in the direction of computer-aided diagnosis using multi-modal views via data fusion. We are conducting experiments towards selecting relevant axial slices and also ways to fuse information from multiple slices. We are also working towards using the axial views in conjunction with the sagittal images to build a robust and fully automatic CAD system.

REFERENCES

[1] Klinder, T., Ostermann, J., Ehm, M., Franz, A., Kneser, R., Lorenz, C., "Automated model-based vertebra detection, identification, and segmentation in ct images.," *Medical Image Analysis* **13**, 471–482 (2009).

[2] S. Ghosh and R. S. Alomari and V. Chaudhary and G. Dhillon, "Automatic lumbar vertebra segmentation from clinical ct for wedge compression fracture diagnosis," in [*Proceedings of SPIE Medical Imaging*], (2011).

[3] M. Tsai and S. Jou and M. Hsieh, "A new method for lumbar herniated inter-vertebral disc diagnosis based on image analysis of transverse sections," *Computerized Medical Imaging and Graphics* **26**(6), 369–380 (2002).

[4] S. Michopoulou and L. Costaridou and E. Panagiotopoulos and R. Speller and G. Panayiotakis and A. Todd-Pokropek, "Atlas-based segmentation of degenerated lumbar intervertebral discs from mr images of the spine," in [*IEEE Transactions on Biomedical Engineering*], **56**(9), 2225–31 (2009).

[5] R. S. Alomari and J. J. Corso and V. Chaudhary and G. Dhillon, "Desiccation diagnosis in lumbar discs from clinical mri with a probabilistic model," in [*Proceedings of IEEE International Symposium on Biomedical Imaging (ISBI)*], 546–549 (2009).

[6] S. Ghosh and R. S. Alomari and V. Chaudhary and G. Dhillon, "Computer-aided diagnosis for lumbar mri using heterogeneous classifiers," in [*Proceedings of the 8th IEEE International Symposium on Biomedical Imaging: From Nano to Macro,ISBI*], 1179–1182 (2011).

[7] S. Ghosh and R. S. Alomari and V. Chaudhary and G. Dhillon, "Composite features for automatic diagnosis of intervertebral disc herniation from lumbar mri," in [*Proceedings of the 33rd Annual International Conference of the IEEE Engineering in Medicine and Biology Society, EMBC*], (2011). to appear.

[8] M. Bhargavan and J. H. Sunshine, and B. Schepps, "Too few radiologists?," *American Journal of Roentgenology* **178(5)**, 1075–1082 (2002).

[9] G. Buirski and M. Silberstein, "The symptomatic lumbar disc in patients with low-back pain: Magnetic resonance imaging appearances in both a symptomatic and control population," *Spine* **18** (1993).

[10] S. Michopoulou and I. Boniatis and L. Costaridou and D. Cavouras and E. Panagiotopoulos and G. Panayiotakis, "Computer assisted characterization of cervical intervertebral disc degeneration in mri," *Journal of Instrumentation* **4**, 287–293 (2009).

[11] Yann Lecun and Lon Bottou and Yoshua Bengio and Patrick Haffner, "Gradient-based learning applied to document recognition," in [*Proceedings of the IEEE*], 2278–2324 (1998).

[12] Jake Bouvrie, "Notes on convolutional neural networks"